LRP 543/96 March 1996

# MEASUREMENT OF THE PARALLEL VELOCITY DISTRIBUTION FUNCTION OF THE ELECTRON BEAM IN A QUASI-OPTICAL GYROTRON BY ELECTRON CYCLOTRON EMISSION

G. Soumagne, S. Alberti, J.P. Hogge,
M. Pedrozzi, M.R. Siegrist,
M.Q. Tran and T.M. Tran

submitted for publication in

PHYSICS OF PLASMAS

# Measurement of the Parallel Velocity Distribution Function of the Electron Beam in a Quasi-Optical Gyrotron by Electron Cyclotron Emission

G. Soumagne, S. Alberti, J.P. Hogge*, M. Pedrozzi,
M.R. Siegrist, M.Q. Tran, and T.M. Tran

Centre de Recherches en Physique des Plasmas,
Association Euratom - Confédération Suisse,
Ecole Polytechnique Fédérale de Lausanne,
21, Avenue des Bains, 1007 Lausanne, Switzerland

## Abstract

The parallel velocity distribution function of the weakly relativistic electron beam of a quasi-optical gyrotron (QOG) has been determined by measuring the Doppler-shifted Electron Cyclotron Emission (ECE) at an angle $\theta = 15°$ with respect to the external magnetic DC-field. Due to the Doppler shift, the frequency of the spontaneous cyclotron emission at the fundamental ($\nu_0 = 100$ GHz) is upshifted to 140 GHz. A broadening of the spectrum up to 10 GHz (Full Width at Half Maximium FWHM) was measured. The measured mean frequency agrees well with the theoretical predictions, but the observed line-width, and hence the parallel velocity distribution function, is $2-3$ times larger than expected. Considerations on ECE-measurements of the electron beam energy spread, performed at larger angles $\theta$, are also discussed.

## I. INTRODUCTION

With the increasing interest in high power mm-wave sources, such as gyrotrons and free electron lasers, beam diagnostics of weakly relativistic and relativistic electron beams has become more and more important. This is due to the fact that the energy coupling between the kinetic energy of the electrons and the electromagnetic energy strongly depends on the "quality" of the electron beam, e.g. its velocity and/or energy spread.

Thomson scattering was used by S.C. Chen [1] to measure the parallel velocity spread and the mean parallel velocity of the relativistic electron beam in a free electron laser. A similar approach on the quasi-optical gyrotron at CRPP was attempted, but had to be abandoned due to mechanical limitation of the set-up [2]. Standard electron beam diagnostics for gyrotrons are mainly performed by capacitive probes and retarding potentials [3,4], but these methods have certain restrictions. Capacitive probes, which are used in situ, provide only information on the linear charge density $\rho$ in the beam. The knowledge of $\rho$ and of the beam characteristics gives the mean parallel velocity. The eventual presence of reflected electrons or of ions in the beam modifies $\rho$ and hence lead to an erroneous determination of the mean parallel velocity. Methods based on retarding potentials, which provide information on the beam parallel velocity spread, require probes which intercept the beam. Therefore, retarding potentials techniques have to be applied on scaled down electron beams. Under these conditions, elctromagnetic instabilities which can be excited by the beam in the beam tunnel are suppressed since the instability frequency is below cut-off. Since such effects deteriorate the electron beam quality, measurements of this type may result in rather optimistic values for the beam quality.

The ECE-diagnostic allows to measure the mean parallel velocity and the parallel velocity spread as well as the corresponding mean electron beam energy and beam energy spreads in situ at full beam parameters. The Doppler shifted frequency $\nu$ emitted by a single electron in the direction $\theta$ with respect to the applied magnetic DC-field is given by:

$$\nu = \frac{\nu_\circ}{\gamma(1 - \beta_\parallel \cos\theta)} \tag{1}$$

where $\nu_\circ$ is the non-relativistic cyclotron frequency, $\gamma$ is the relativistic factor and $\beta_\parallel = v_\parallel/c$ the normalized parallel velocity. The frequency depends on the energy and the parallel velocity of the electron. The measurement of the ECE-spectrum of an electron beam, consisting of an ensemble of electrons, contains therefore the information on energy and parallel velocity spreads. Depending on the viewing angle $\theta$ the spectrum can either be more sensitive to the electron beam energy ($\theta \simeq 60^0$) or to the parallel velocity ($\theta \simeq 15^0$) spreads. In order to determine the parallel velocity distribution function, measurements have been performed at an angle $\theta = 15°$ where the spectrum is determined by the parallel velocity spread. The observed frequency upshift is about 40 GHz for our beam parameters. The spectrum is outside the spectral region of the relativistic cyclotron frequency, where parasitic oscillations have also been observed ($f \simeq 100\,\mathrm{GHz}$) [5]. A preliminary experiment was performed by Alberti et al. [6] and other results were reported by Soumagne et al. [7].

The paper is structured as follows: A brief introduction of the theory is given, followed by the description of the experimental set-up. Finally, the main experimental results will be discussed and summarized.

## II. THEORETICAL ASPECTS

In order to calculate the spectral power density of the spontaneous electron cyclotron emission of the electron beam, Maxwell's equations are solved first for a single electron. For

an arbitrary electron trajectory, the solution is given by the Lienard-Wiechert potentials (see e.g. [8]). Note, that the Lienard-Wiechert potentials are free space solutions whereas the ECE is generated inside the gyrotron vessel. The inner dimension of our vacuum vessel is, however, much larger than the emitted wavelength. It therefore represents a highly overmoded waveguide and the free space solution remains valid in this case as shown by Haus et al. [9].

Due to the applied external magnetic DC-field the electron trajectory inside the gyrotron is helical. A detailed derivation of the the total emitted power for this type of trajectory can be found in Hutchinson [10]. For our experimental parameters several approximations can be made. First, only the fundamental harmonic was considered because most of the power ($\simeq 70\,\%$) is generated in the fundamental for the given electron beam. Second, the electron beam is only weakly relativistic and orders higher than $\beta^2$ are therefore omitted in the polynomial development of the Bessel function. Third, only the y-polarization (Fig. 1) of the electric field has been taken into account due to the orientation of the rectangular waveguide used for the ECE detection. Within these approximations, for one electron, the total emitted power per solid angle $d\Omega_s$ is given by:

$$\frac{dP'}{d\Omega_s} = \frac{e^2\nu_\circ^2}{8\epsilon_\circ c}\frac{\beta_\perp^2}{(1-\beta_\parallel\cos\theta)^3}\,, \tag{2}$$

where $e$, $\epsilon_\circ$ and $c$ are the electron charge, the vacuum permittivity and the speed of light respectively. Note, that the emitted power $dP'/d\Omega_s$ is related to the received power $dP/d\Omega_s$ by:

$$\frac{dP'}{d\Omega_s} = \frac{dP}{d\Omega_s}\,(1-\beta_\parallel\cos\theta)\,. \tag{3}$$

For the typical beam parameters and by considering only the y-polarization, the angular distribution of the emitted power per solid angle is shown in Fig. 1. One notices that even for weakly relativistic beams ($\beta_\parallel = 0.3$, $\gamma = 1.137$) there is an angular asymmetry in the radiated power with an important emission in the forward direction.

No coherence exists between the electrons in the absence of cyclotron maser instability (the cavity had been removed during the experiment) and the total emitted power of the electron beam is therefore the sum of the emitted power of all electrons. In addition, due to the low electron density of $10^{17}\,\mathrm{m}^{-3}$ the self-absorption of the electron beam, which is proportional to $\nu_p^2/\nu_\circ$ [10], is negligible. Hence, the electron plasma is optically thin and the emitted spectrum is not modified by the beam. The emitted spectral power density of the electron beam can therefore be written as:

$$\frac{d^3P'}{d\nu d\Omega_s dV} = \frac{n_e e^2}{8\,\epsilon_\circ c}\,\nu^2\,\beta_\perp^2\,\delta\left[\left(1-\beta_\parallel\cos\theta\right)\nu - \nu_\circ/\gamma\right] \tag{4}$$

where $n_e$ is the electron density.

Due to the helical motion of the electrons, a general velocity distribution function is of the form $f(\beta_\perp, \beta_\parallel)$. In the special case of a monoenergetic beam with $\gamma \equiv \gamma_\circ$, both velocity components are related by:

$$\beta_\perp = \sqrt{1-\gamma_\circ^{-2}-\beta_\parallel^2}\,. \tag{5}$$

and the velocity distribution function is only a function of one of the two velocity components. Assuming that the parallel velocity is the independent parameter, the received spectral power density can be written as:

$$\frac{d^3P}{d\nu d\Omega_s dV} = \frac{n_e e^2 \nu^2}{8\,\epsilon_o c} \int \frac{\beta_\perp^2}{1-\beta_\parallel \cos\theta}\, f(\beta_\parallel)\, \delta\left[\left(1-\beta_\parallel\cos\theta\right)\nu - \frac{\nu_o}{\gamma_o}\right] d\beta_\parallel$$

$$= \frac{n_e e^2}{8\,\epsilon_o c}\,\frac{\nu}{\cos\theta}\,\frac{1-\gamma_o^{-2}-\beta_\parallel^2(\nu)}{1-\beta_\parallel(\nu)\cos\theta}\, f\left[\beta_\parallel(\nu)\right] \tag{6}$$

with:

$$\beta_\parallel(\nu) = \frac{1}{\cos\theta}\left(1-\frac{\nu_o}{\gamma_o\,\nu}\right). \tag{7}$$

Based on Eq. 6, the received spectral power density for a Gaussian velocity distribution function $f(\beta_\parallel)$ at $\theta$=15° is plotted in Fig. 2. As one can see, the spectrum is entirely determined by the velocity distribution function $f(\beta_\parallel)$.

If the electron beam has a certain energy spread $\delta\gamma = \Delta\gamma/<\gamma>$ (where $<\gamma>$ is the mean value and $\Delta\gamma$ is the RMS spread) due to parasitic oscillations in the drift tube and that $\gamma$ and $\beta_\parallel$ are independent variables, the received spectral power density can be written as:

$$\frac{d^3P}{d\nu d\Omega_s dV} = \frac{n_e e^2 \nu^2}{8\,\epsilon_o c} \iint \frac{\beta_\perp^2}{1-\beta_\parallel \cos\theta}\, g(\gamma)\, f(\beta_\parallel)\, \delta\left[\left(1-\beta_\parallel\cos\theta\right)\nu - \frac{\nu_o}{\gamma}\right] \frac{2\,\pi}{\gamma^3} d\gamma\, d\beta_\parallel$$

$$= \frac{\pi\, n_e e^2}{4\,\epsilon_o c}\,\frac{\nu}{\cos\theta} \int \frac{1-\gamma^{-2}-\beta_\parallel^2(\gamma,\nu)}{1-\beta_\parallel(\gamma,\nu)\cos\theta}\,\frac{1}{\gamma^3}\, g(\gamma)\, f[\beta_\parallel(\gamma,\nu)]\, d\gamma \tag{8}$$

with:

$$\beta_\parallel(\gamma,\nu) = \frac{1}{\cos\theta}\left(1-\frac{\nu_o}{\gamma\,\nu}\right). \tag{9}$$

From Eq.8 the dependency of the relative spectral width, $\delta\nu$, on the energy, $\delta\gamma$, for a fixed parallel velocity spread of $\delta\beta_\parallel = \Delta\beta_\parallel/<\beta_\parallel>= 10\,\%$, as a function of the observation angle $\theta$ is shown in Fig.3. Both distributions in $\beta_\parallel$ and $\gamma$ were gaussian. As one can see, for shallow angles ($\theta \simeq 15^0$) the ECE spectrum width is mainly sensitive on parallel velocity spread, whereas at larger angles ($\theta \simeq 60^0$) it is sensitive on energy spread. From Eq.8 the sensitivity of the spectral peak power value as a function of the observation angle, $\theta$, for different relative widths of the distribution functions of the parallel velocity $\delta\beta_\parallel$, and different energy spreads $\delta\gamma$ is shown in Fig. 4. For viewing angles smaller than $\theta = 60°$, the peak value is fairly insensitive to parallel velocity and energy spreads.

As it will be discussed later, it is important to note that if instabilities are excited in the beam duct before the diagnosed region, the energy distribution function might deviate significantly from the supposed gaussian shape and that values of $\delta\gamma$ larger than 1.5% are very unlikely and are shown here only as example. The simultaneous determination of the parallel velocity spread and the energy spread, requires measurements at two different angles.

## III. EXPERIMENTAL SET-UP

A schematic of the quasi-optical gyrotron is given in Fig. 5 and a detailed description of the gun and magnetic configuration can be found in Ref. [11]. The laminar electron beam is produced by a triode magnetron injection gun (MIG). The electrons emitted from the temperature limited cathode are accelerated, adiabatically compressed by the applied magnetic DC-field (compression $\simeq 20$) and guided from the MIG to the interaction region

where the Fabry-Perot resonator is placed. The resonator axis is perpendicular to the beam propagation, so that in the interaction region, the electron beam is not confined by any closed metallic boundary. For this experiment, the oscillation on a resonator mode was prevented by inserting in front of the mirrors an absorbing material (Macor). This "free propagation" region of the electrons allows to measure the spontaneous ECE at a chosen angle $\theta$. After passing the interaction region, the electron beam is guided to a collector. Due to experimental limitations, the beam current could not be set at values higher than 4.5A. A capacitive probe was located in the beam duct just before the free propagation region as shown in Fig. 6.

The experimental set-up for the ECE measurement is shown in Fig. 6. The angle $\theta$ is fixed at 15° and as it was shown in Fig. 3, the ECE spectrum will mainly be determined by parallel velocity spread. The Doppler-shifted ECE is collected by a WR-06 horn inside the gyrotron and guided to the outside of the vessel. The received signal goes through a high pass filter (cut-off frequency, $f_c = 116$GHz) which rejects parasitic oscillations excited in the gyrotron beam tunnel observed at $\simeq 100$ GHz. Finally, the ECE-signal is downconverted by a heterodyne detector operating at the fundamental to an intermediate frequency (IF) of $8-12$ GHz, which is amplified and filtered with two band-pass filters at 8.0 and 8.5 GHz ($\pm 50$ MHz). The typical collected peak power in a frequency band of 100MHz around 140GHz is -56dBm.

The relative calibration of the detection system was performed by two methods. A black-body source (Eccosorb) at two different temperatures ($T = 300^0$K and $T = 77^0$K) was used. An in-situ calibration using the electron beam was also applied. In the latter case, the spectrum was shifted by changing the electron beam parameters such that the mean IF-frequency was finally placed between 8.0 and 8.5 GHz for each applied LO-frequency. Since the spectrum is symmetric and much larger than 0.5 GHz, the ratio of the amplitudes of both filters gives a relative calibration. An agreement of $\pm 0.5$ dB between both methods was found.

In order to measure the whole spectrum, the frequency of the local oscillator (LO) is changed by 1 GHz from shot to shot. As the frequency of the LO is fixed during a gyrotron shot, time resolved spectra can be obtained.

## IV. EXPERIMENTAL RESULTS

A measured ECE-spectrum is shown in Fig. 7 (dashed line). Each point represents the average of three measurements at constant LO-frequency. The whole spectrum has been measured by successively increasing the LO-frequency from 122.0 to 140.0 GHz in steps of 1.0 GHz. The spectrum based on the beam parameters in the interaction region calculated by the electron beam trajectory code DAPHNE [12] is also presented for comparison. For the calculated spectrum, the parallel velocity distribution function was assumed to be gaussian and several broadening effects as space charge depression [13], electron time of flight in the detection region and the antenna gain function were included. We have also assumed no energy spread ($\delta\gamma = 0$). For the 15° viewing angle, the main broadening effect is due to electron time of flight (0.6 GHz), and the overall broadening is of the order of (1 GHz) . The mean frequencies are in good agreement, whereas the measured width of the spectrum is 3.3 times larger than the the value predicted by the trajectory code DAPHNE.

The dependency of the calculated and measured (ECE and capacitive probe) mean perpendicular velocity $<\beta_\perp>$ as a function of the modulation voltage, $V_{mod}$, is shown in Fig. 8 for a beam voltage $V_c$ of $-62.0$ kV and a beam current of 1.5 A. A good agreement is found

between the values deduced from the two experimental methods and the value calculated with the trajectory code.

For the same experimental conditions of Fig. 8, the dependency of the calculated and measured perpendicular velocity spreads versus modulating voltage is shown in Fig. 9. The perpendicular velocity spread $\delta\beta_\perp$ has been calculated by assuming a monoenergetic beam $\delta\gamma = 0$ which allows to relate the measured $\delta\beta_\parallel$ to $\delta\beta_\perp$ by :

$$\delta\beta_\perp = \frac{\Delta\beta_\perp}{<\beta_\perp>} = \frac{1}{\alpha^2}\frac{\Delta\beta_\parallel}{<\beta_\parallel>} \tag{10}$$

This same relation is usually taken for diagnostics based on the retarding potential technique [17]. The assumption of a monoenergetic beam is related to the fact that trajectory codes do not take into account any AC effects, and the only source of energy spread in these codes is due to DC self-fields within the electron beam, which is usually negligible. As one can observe in Fig. 9, for a modulation voltage smaller than 30 kV, $\delta\beta_\perp$ remains always 2 – 3 times larger than the theoretical values. This observation agrees with measurements obtained with a retarding potential technique [17].

Time resolved measurements allowed to observe a space charge neutralization effect within the observation volume. Fig. 10 represents the mean emitted frequency of the measured spectrum as a function of time for a beam current of 4.5 A. For reference, a typical trace of the modulation voltage, $V_{mod}$, is shown. All other characteristic parameters ($\gamma$, $I_b$) remain constant and the ECE frequency should therefore remain constant as shown by the theoretical curve in Fig. 10. The measured frequency increase may be due to an increase of the mean parallel velocity caused by a partial space charge neutralization of the beam which reduces the potential depression in the interaction region. The ionization cross section for the considered electron beam energy of 62 keV and a molecule of the background gas is fairly independent of the typical atom species ($O_2$, $N_2$,$H_2O$) and a value for $N_2$ is $\sigma_i = 2.65\ 10^{-22}$ m$^2$ [18]. For the working background pressure of $10^{-6}$ mbar in the vacuum vessel the typical ionization time $\tau_n = 1$ ms ($\tau_n = 1/n_g\sigma_i v$, where $n_g$ is the background gas density and $v$ is the total electron velocity) is in a good agreement with the experimental measurements. This observation is consistent with independent measurements made with a capacitive probe (Fig. 11). The amplitude of the capacitive probe signal also shows a significant decrease as a function of time which is consistent with the assumption of space charge neutralization.

## V. DISCUSSION

Part of the difference between theory and measurement can be attributed to the surface roughness effects of the cathode surface, an effect not taken into account in the trajectory code DAPHNE. The surface roughness generates only velocity spread with no energy spread, and as it has been shown by different authors [14,15], that a cathode surface roughness of 2 $\mu$m results in a perpendicular velocity spread of 6 % [14]. This effect in addition to other perturbating ones have been implemented in a trajectory code by Lygin [16] which, by using a retarding potential technique, shows that depending on the beam current, initial velocity spreads at the emitter can cause an important deviation of the distribution function from a gaussian shape. It is important to remark that the parallel velocity distribution function is directly related to the ECE spectrum (Eq. 6): which implies that a more complicated structure than a gaussian would then be observed in the ECE spectrum. In our experiment such deviations of the distribution function were not found.

As it was discussed earlier, in this experiment the ECE spectrum is mainly determined by the parallel velocity spread and not by energy spread. However excitation of parasitic oscillations in the beam tunnel has been observed by Pedrozzi et al. [5]. This suggests the existence of an energy spread. An estimation of the energy spread generated by such oscillations based on a linear theory shows that an energy spread $\delta\gamma$ ranging between 0.4 and 0.8% is to be expected. Such values of $\delta\gamma$ can importantly reduce the gyrotron efficiency as it is shown in Fig. 12 where the example of a Quasi-Optical gyrotron is taken [11].

One observes in this figure that the gyrotron efficiency is strongly affected by $\delta\gamma$ whereas the dependence on $\delta\beta_{\|}$ is weak. This is due to the fact that the gyrotron interaction is strongly dependent on the detuning parameter, $\Delta f_g/f_g = 1-\nu_0/\gamma f_g$ which is itself dependent on $\gamma$ ($f_g$ being the gyrotron RF frequency). Without a measurement of $\delta\gamma$, the value of $\delta\beta_{\perp}$ cannot be inferred from the present set-up. Consequently, an additional ECE-measurement at a larger angle $\theta \simeq 60°$ is required (see Fig. 3) in order to simultaneously obtain energy and parallel velocity spreads.

## VI. CONCLUSION

It has been shown that ECE can be used to measure the parallel velocity distribution function of a weakly relativistic electron beam. The measured spectrum at $\theta = 15°$ depends on the parallel velocity distribution function only. Whereas measured widths are significantly larger than the value predicted by the electron gun code DAPHNE, mean values agree in general very well. The measured parallel velocity spread is consistent with the value obtained by considering a cathode surface roughness of 2 $\mu$m. Time resolved measurements allowed the observation of space charge neutralization effects.

To confirm our interpretation, an additional ECE-measurement at a larger angle $\theta$ is required in order to simultaneously obtain energy and parallel velocity spreads.

## VII. ACKNOWLEDGMENTS

This work was partially supported by the Office Fédéral de l'Energie under grants OFEN-EF-FUS(91)-01 and OFEN-Gyrotron 581 233, and by the Fonds National Suisse pour la Recherche Scientifique.

# REFERENCES


* Present address: Plasma Fusion Center, Massachusetts Institute of Technology, Cambridge, 02139 MA.

[1] S.C. Chen and T.C. Marshall, Phys.Rev.Lett. **52**, 425 (1984).

[2] M.R. Siegrist, G. Soumagne and M.Q. Tran, J. Appl. Phys., **74**(4), 2229 (1993).

[3] W.C. Guss et al., J. Appl. Phys. **69**(7), 3789 (1991).

[4] B. Piosczyk, in *Proceedings of 17th International Conference on Infrared and Millimeter Waves*, Pasadena 1992, SPIE **1929**, 494 (1992).

[5] M. Pedrozzi, S. Alberti and M.Q. Tran, in *Proceedings of 20th International Conference on Infrared and Millimeter Waves*, Waves, Orlando 1995, 134 (1995).

[6] S. Alberti et al. in *Proceedings of 14th International Conference on Infrared and Millimeter Waves*, Würzburg 1989, SPIE **1240**, 535 (1989).

[7] G. Soumagne et al. in *Proceedings of 19th International Conference on Infrared and Millimeter Waves*, Sendai 1994, JSAP Catalog No: AP 941228, 468 (1994).

[8] J.D. Jackson, Classical Electrodynamics, chapter 14, John Wiley and Sons, New York, 1975.

[9] H.A. Haus and M.N. Islam, J. Appl. Phys. **54**(9), 4784 (1983).

[10] I.H. Hutchinson, Principles of Plasma Diagnostics, chapter 5, Cambridge University Press, New York, 1987.

[11] S. Alberti et al., Phys. Fluids **B2**, 1654 (1990).

[12] T.M. Tran et al.,in *Proceedings 6th joint EPS-APS International Conference on Physics Computation*, Lugano 1994, PC94, 491 (1994).

[13] S. Alberti et al., Phys. Fluids **B3**, 519 (1991).

[14] Sh.E. Tsimring Radiophys. Quantum Electron. **15**(8), 952 (1972).

[15] Y.Y. Lau, J. Appl. Phys. **61**(1), 36 (1987).

[16] V.K. Lygin, Int. J. Infrared Millimeter Waves **16**, 363 (1995).

[17] B. Piosczyk,in *Proceedings of 18th International Conference on Infrared and Millimeter Waves*, Colchester 1993, SPIE **2104**, 450 (1993).

[18] F.F. Rieke and W. Prepejchal, Phys.Rev.A **6**(4), 1507 (1972).

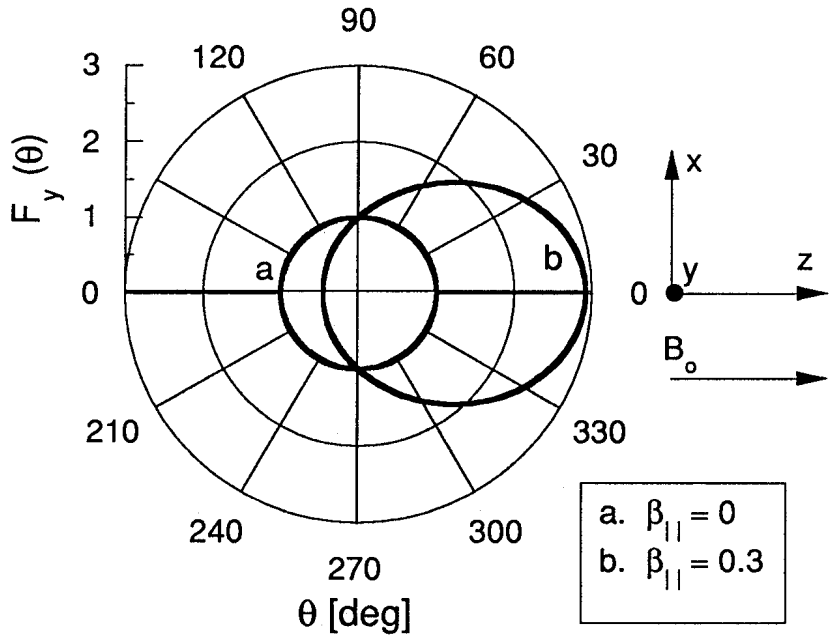


FIG. 1. Angular distribution of radiated power per solid angle in the y-polaization for $\beta_{||} = 0$ (curve a) and for $\beta_{||} = 0.3$ (curve b).

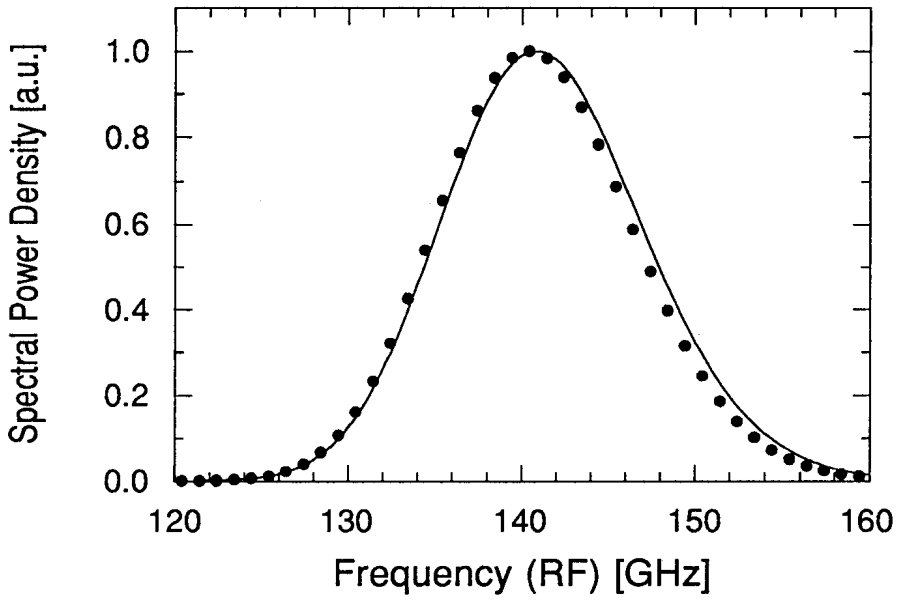


FIG. 2. Normalized spectral power density of ECE (dots). Continuous line: parallel velocity distribution function $f(\beta(\nu))$. Other parameters are: $<\beta_{\|}>= 0.282$, $<\gamma>= 1.117$, $\nu_0 = 100$GHz, $\theta = 15^0$.

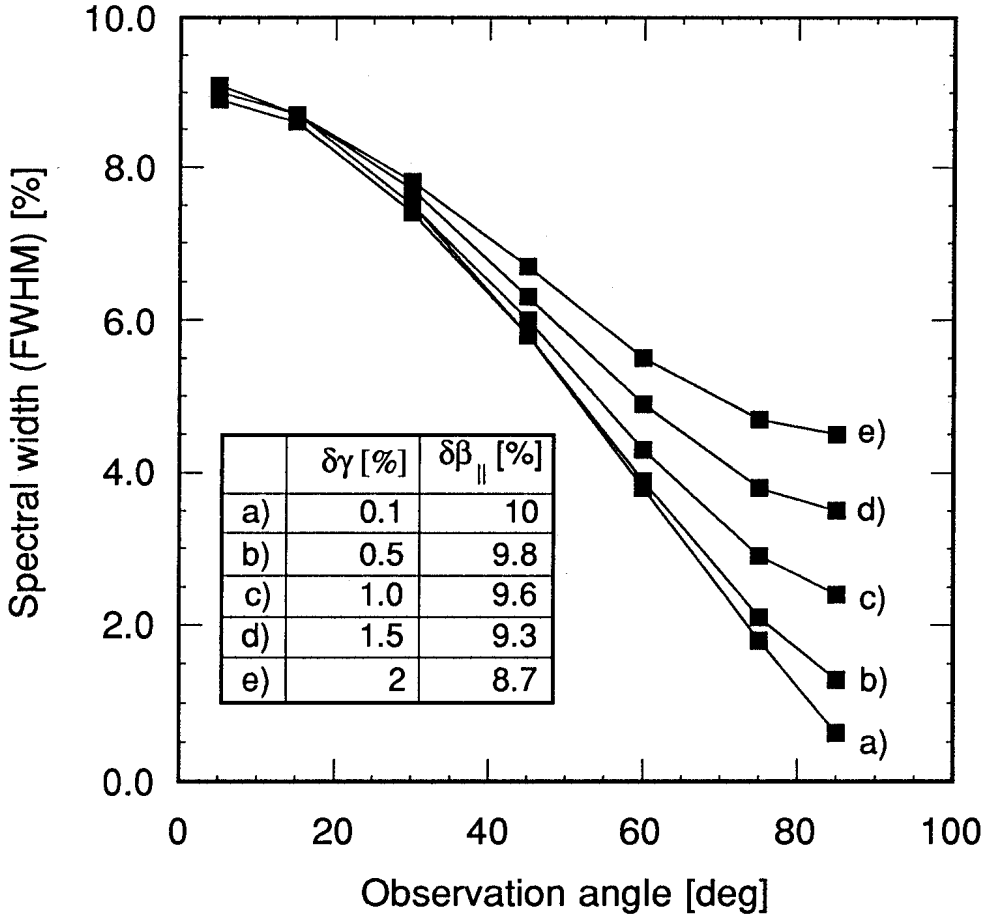


FIG. 3. Relative spectral width of the ECE-spectrum as a function of the observation angle, $\theta$, for different relative widths of the distribution functions of the parallel velocity $\delta\beta_{\|}$, and different energy spreads $\delta\gamma$. The spectral width at $\theta = 15^o$ is fixed at 8.7%, the mean parallel velocity is $< \beta_{\|} >= 0.282$ and the mean energy $< \gamma >= 1.117$.

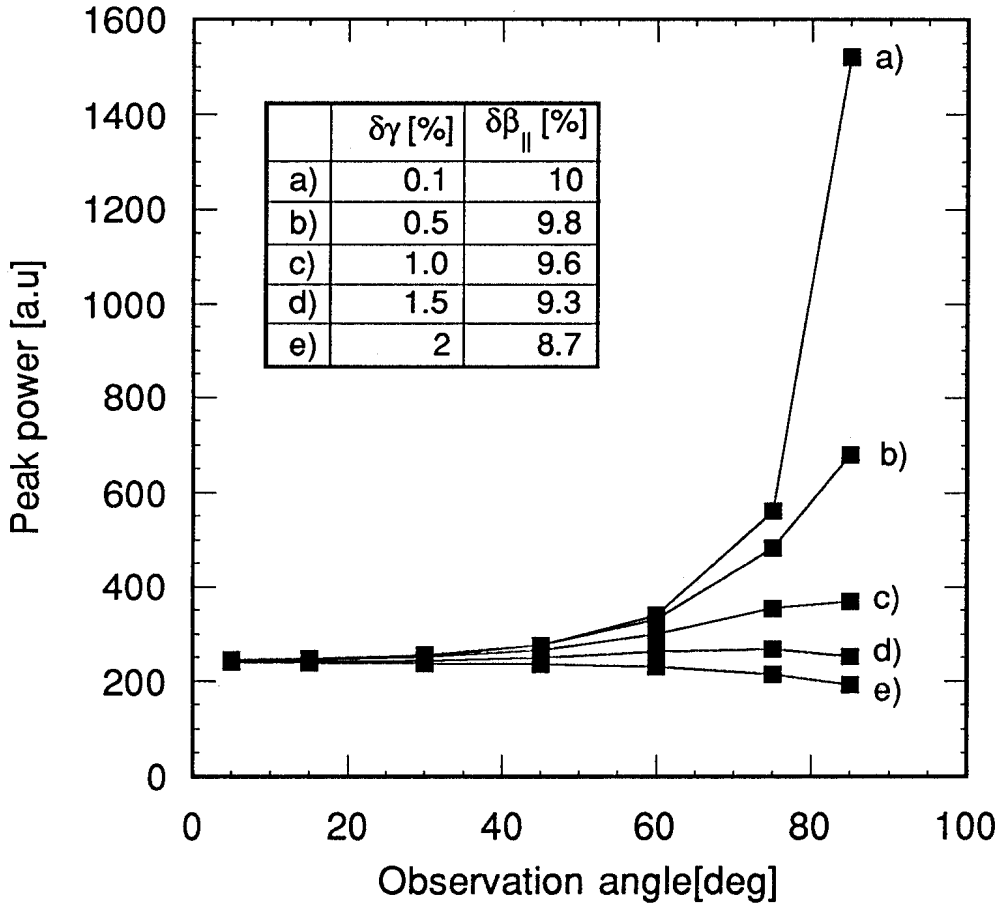


FIG. 4. Peak power as a function of the observation angle, $\theta$, for different relative widths of the distribution functions of the parallel velocity $\delta\beta_{\|}$, and different energy spreads $\delta\gamma$. The mean parallel velocity is $< \beta_{\|} >= 0.282$ and the mean energy $< \gamma >= 1.117$. The electron density is kept constant.

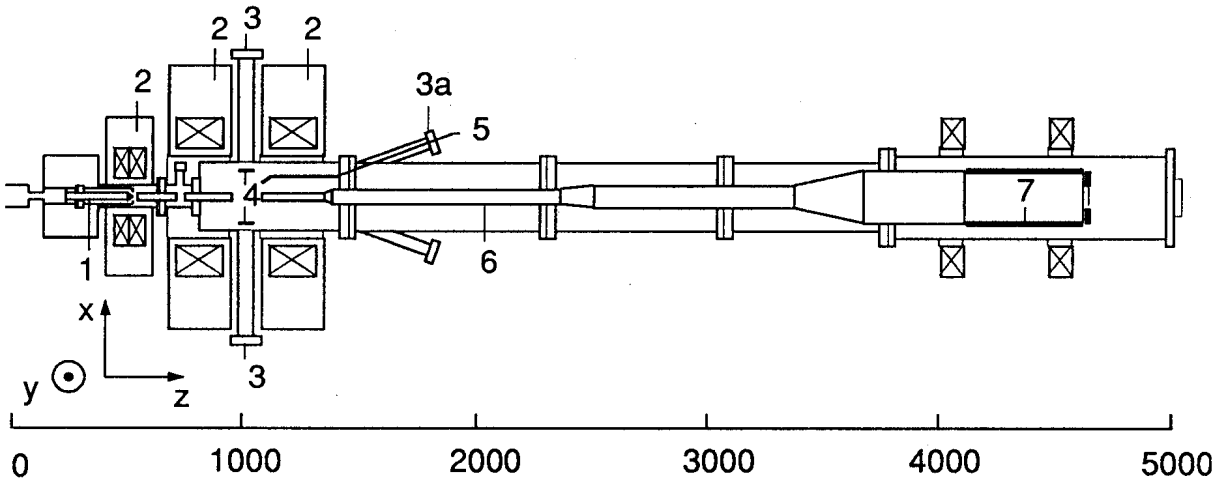


FIG. 5. Schematic of the quasi-optical gyrotron. 1: MIG Electron Gun; 2: Magnetic Coils; 3: RF-Window; 4: Observed Region; 5: Waveguide (ECE-experiment); 6: Beam Tunnel; 7: Collector.

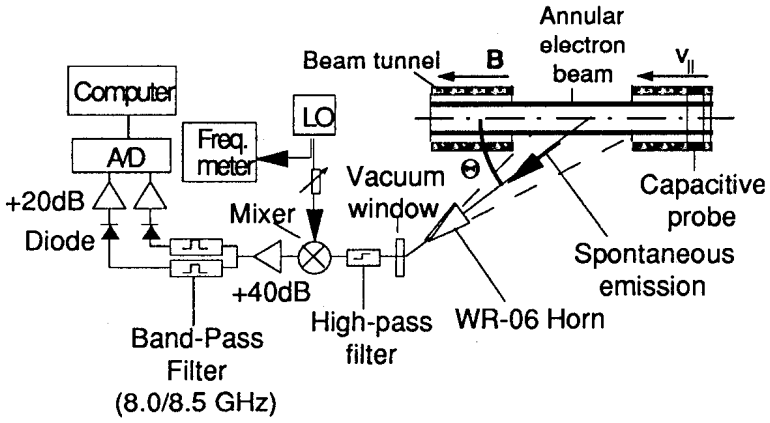


FIG. 6. Schematic of ECE measurement experimental set-up.

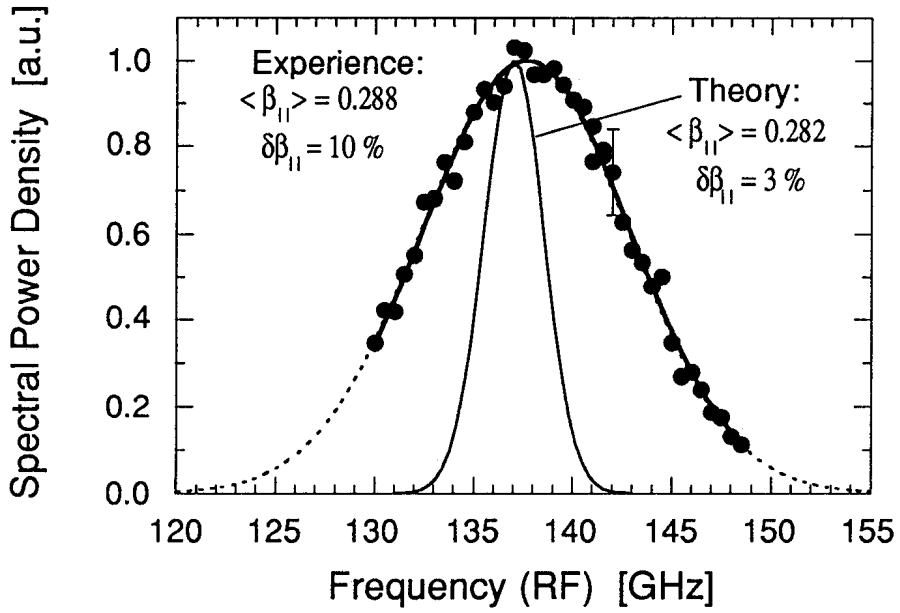


FIG. 7. Experimental (dashed) and calculated (line) spectrum. Electron beam parameters: $V_c = -62.0\,\mathrm{kV}$; $V_{mod} = +28.8\,\mathrm{kV}$; $I_b = 1.5\,\mathrm{A}$.

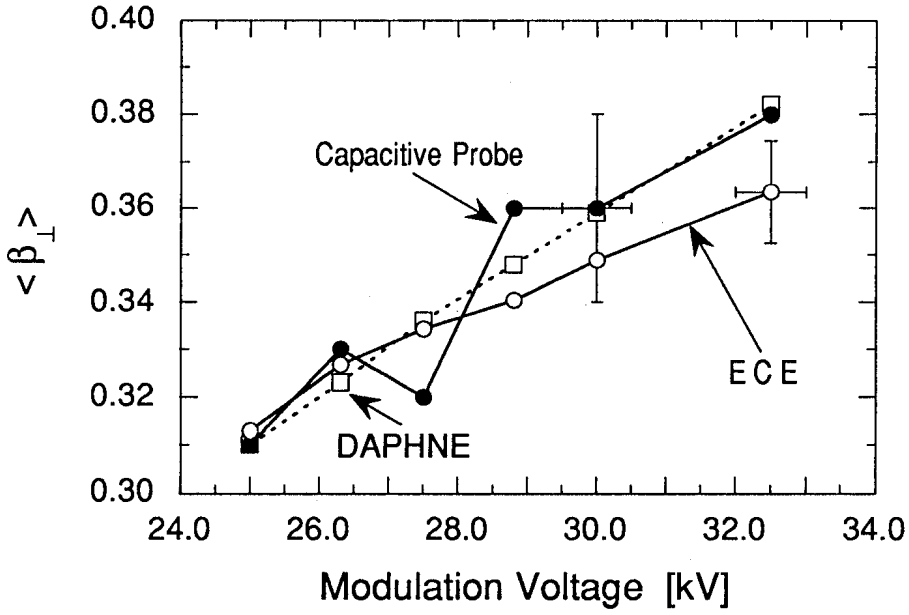


FIG. 8. Mean perpendicular velocity $<\beta_\perp>$ deduced from the capacitive probe (•) and from the ECE (○) as a function of the anode voltage $V_{mod}$. $V_c = -62.0\,\mathrm{kV}$; $I_b = 1.5\,\mathrm{A}$. Also shown are simulation results obtained with DAPHNE (2).

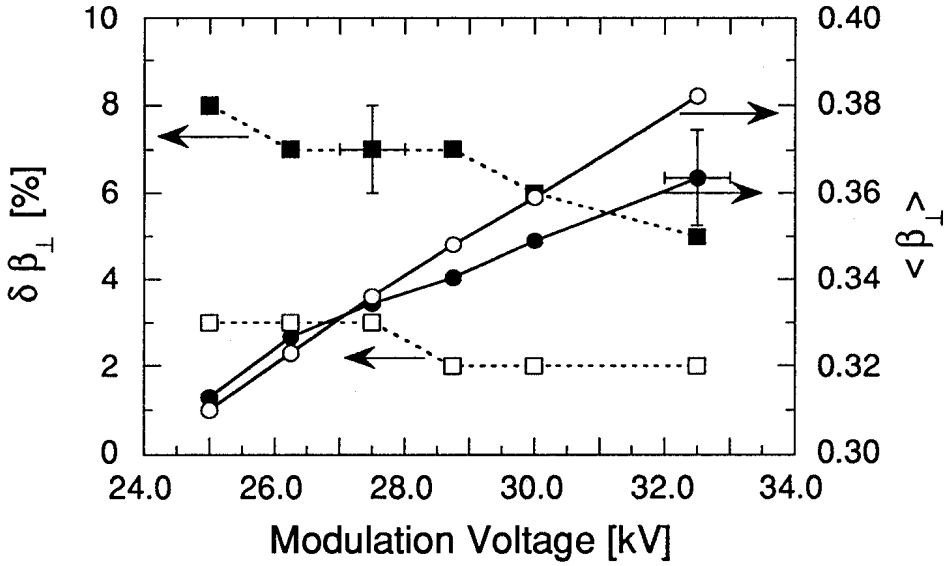


FIG. 9. Mean perpendicular velocity $<\beta_\perp>$ and perpendicular velocity spread $\delta\beta_\perp$ as a function of the modulation voltage $V_{mod}$. $V_c = -62.0\,\mathrm{kV}$; $I_b = 1.5\,\mathrm{A}$. Experiment: closed symbols; Theory: open symbols.

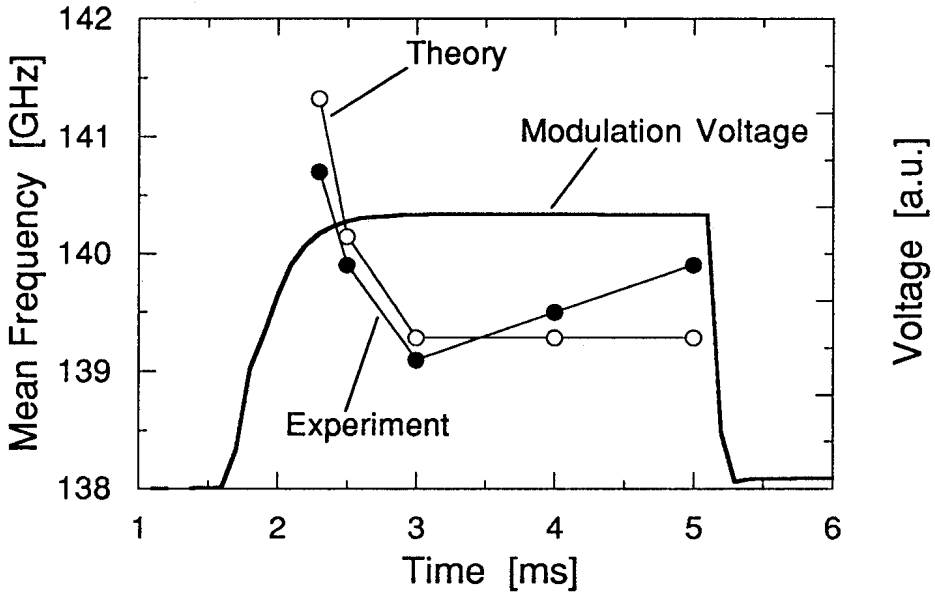


FIG. 10. Temporal evolution of the mean frequency of the ECE-spectrum and a typical trace of the modulation voltage; cathode voltage: −62.0 kV; modulation voltage: 27.5 kV, beam current: 4.5 A.

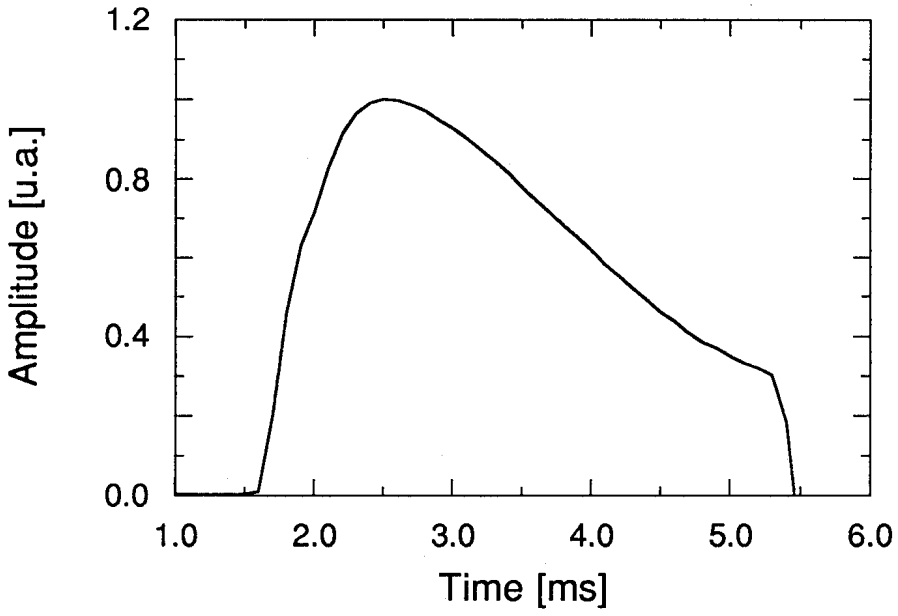


FIG. 11. Temporal evolution of the capacitive probe signal; cathode voltage: −62.0 kV; modulation voltage: 27.5 kV, beam current: 4.5 A.

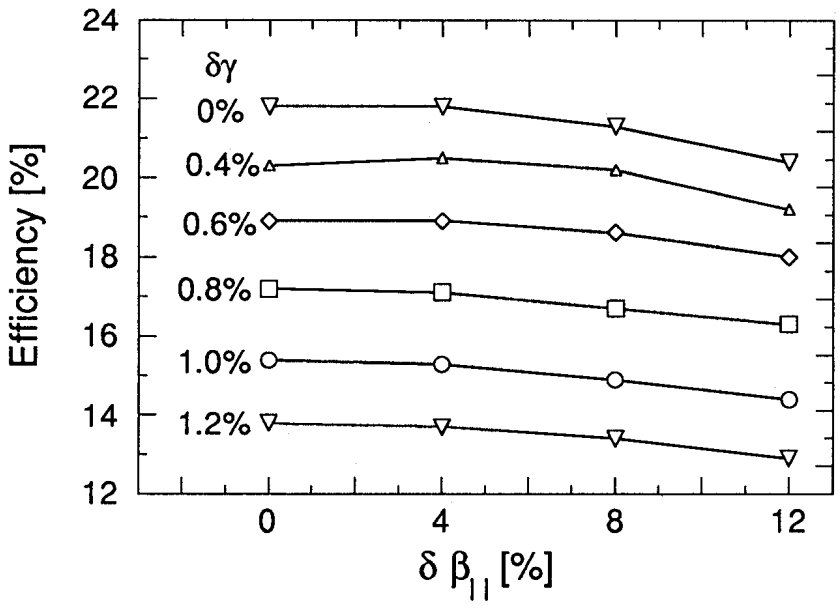


FIG. 12. Calculated efficiency of the QOG as a function of the relative width of the distribution function of the parallel velocity, $\delta\beta_{\|}$, and the relativistic factor, $\delta\gamma$.